COMPOSITIONAL CHARACTERIZATION OF IRREGULAR MARE PATCHES VIA M^3 AND DIVINER DATA ANALYSES. N. Piskurich[1], K. L. Donaldson Hanna[1], M. Martinot[1], B. T. Greenhagen[2], [1]Dept. of Physics, University of Central Florida, Orlando, FL (npiskuri@knights.ucf.edu), [2]Johns Hopkins Applied Physics Laboratory, Laurel, MD.

Introduction: Irregular mare patches (IMPs) are small to mesoscale (~15 – 5000 m maximum length) hypothesized volcanic features on the lunar nearside that occur primarily in host mare settings [1, 2, 3]. IMPs are characterized by two morphologically distinct deposits: bulbous-shaped, smooth mounds with uniform texture and little to no blocks/boulders, and surrounding optically immature deposits with rough surface textures and a range of block densities [4, 5]. The discovery and geological characterization of the first IMP feature known as Ina in 1972 from Apollo 15 photographs has led to an ongoing debate about their origins and formation mechanisms [e.g., 3, 6]. Recent morphologic Lunar Reconnaissance Orbiter Camera (LROC) observations coupled with crater counting have suggested that the IMPs may be relatively recent features (~ 10 – 100 Ma) [4].

Numerous formation mechanisms for IMPs have been proposed, including sublimation [3], small lava intrusions and caldera collapse [1], episodic outgassing and removal of surface regolith within the past 10 Ma [7], lava flow inflation [8], small basaltic eruptions within the past 100 Ma [4], pyroclastic eruptions [9], and lava lake processes and magmatic foam extrusions [10].

Here we characterize compositional trends in the four largest IMPs that will allow us to better discriminate between IMP formation scenarios. Compositional characterization of IMPs will give insight into the Moon's thermal evolution and provide constraints for thermochemical or geophysical models of the lunar interior.

Methodology: Compositional characterization is performed for the IMPs that exhibit the largest spatial extents: Sosigenes (8.335°, 19.071°), Ina (18.65°, 5.30°), Cauchy-5 (7.169°, 37.592°), and Maskelyne (4.33°, 33.75°), with maximum lengths of ~ 5000 m for Sosigenes and ~ 3000 m for the latter three features. The compositional data compiled for these IMPs will be compared to their surrounding terrains (e.g., host mare settings) to investigate their similarities and differences. Moon Mineralogy Mapper (M^3) Level 2 observations (~ 0.4 – 3 μm, 85 spectral channels, and ~ 140 – 280 m spatial resolution) were used to identify prominent absorption bands for the IMPs and the spectral parameters that best distinguish the IMPs from their surroundings (e.g., band depth, band center, band ratios).

Initial analyses of the four largest IMPs indicated compositions consistent with pyroxenes (i.e., spectra with absorptions near 1- and 2-μm due to the occupancy of Fe^{2+} in the M1 and M2 crystallographic sites), so we applied the parabolas and two-part linear continuum (PLC) algorithm [12] to the M^3 spectra. In order to smooth the spectra, a Savitzky-Golay filter was applied by fitting a 5th order polynomial to every 13 reflectance values. To compute the band center positions (a parameter indicative of compositional variation), interpolated reflectance values were computed for wavelength ranges with higher resolution (e.g., 0.05 μm step size), and 4th order polynomials were fit to both the band 1 and band 2 regions. Several subgroups of geologic interest were analyzed within and surrounding each IMP: smooth mounds, hummocky terrain, an average of each IMP, surrounding regolith, low albedo craters, and fresh high albedo craters. For each subgroup, an arithmetic average was computed based on the number of regions collected. In Fig. 1A, we show an example M^3 reflectance band and the locations of the collected subgroup spectra (Maskelyne is outlined in green). Average and continuum-removed spectra using the PLC routine for Maskelyne are shown in Figs. 1B and 1C.

Multispectral thermal infrared observations from the Diviner Lunar Radiometer (Diviner) (~ 0.3 – 400 μm, 9 spectral channels, ~ 200 m spatial resolution) were used in conjunction with M^3 spectral measurements. Diviner's three channels near 8 μm (7.81 μm, 8.28 μm, and 8.55 μm) [12] were used to map the Christiansen feature (CF) in silicate minerals. Wavelength positions of the CF correlate to the degree of polymerization of minerals as well as bulk composition, and the common rock-forming lunar minerals (i.e., feldspar, pyroxene, and olivine) exhibit variable CF positions [13]. Corrected Christiansen feature (cCF) (i.e., photometrically corrected via projection onto a topographic grid, corrected for photometric geometry, and modified by the empirical correction methodology "CX3" that normalizes the data to equatorial noon [after 12] maps for Maskelyne between 7:00 – 17:00 local lunar time are shown in Fig. 2.

Discussion: Characterization of M^3 spectra of Ina and Sosigenes corroborates previous results [14, 15] suggesting that the strongest ferrous absorption bands are displayed by the brighter, blockier, and optically immature floor materials. On the contrary, Maskelyne's smooth mounds (more optically mature) exhibit the deepest band depths.

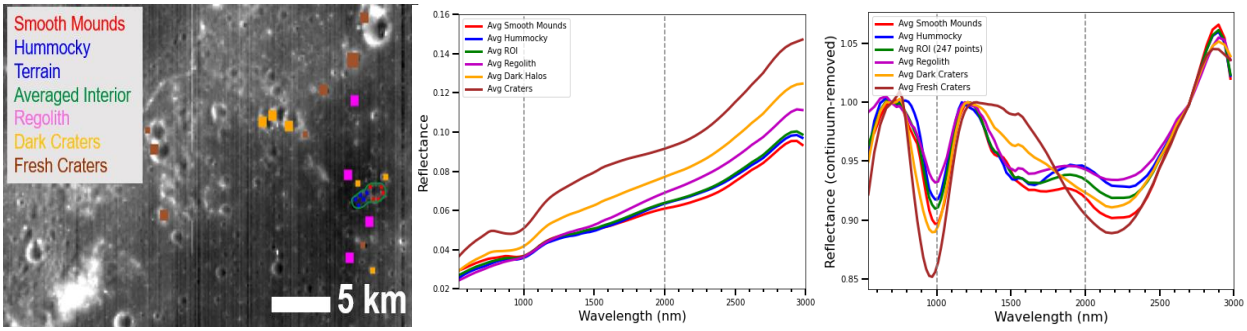

Figure 1: (A) M^3 M320090203T041059 band 5 (620.69 nm), Optical Period 1B (~140 m/pixel). **(B)** M^3 Maskelyne average spectra of units identified in (A). **(C)** Continuum-removed spectra of the same units.

As seen in Figs. 1B and 1C, average spectra for Maskelyne's interior are generally similar to the average spectra of nearby subgroups. The interior spectra of Maskelyne tend to show absorption band centers at longer wavelengths than the surrounding regolith, dark craters, and fresh craters. Maskelyne's interior spectra are similar to the surrounding regolith. Maskelyne's interior is outlined in black on the Diviner cCF map in Fig. 2. Maskelyne's interior exhibits CF values between 8.20 – 8.30 µm, which is consistent with laboratory spectra of Apollo mare basaltic soils that have CF values between ~ 8.10 – 8.35 µm [e.g., 16]. The host mare basalts surrounding Maskelyne exhibit CF positions at longer wavelengths, between ~ 8.35 – 8.45 µm. The shift in the CF position between the interior and exterior of Maskelyne is ~ 0.1 µm, which is consistent with CF variations between mature and immature basaltic surfaces of similar composition [17]. The low albedo craters northwest of Maskelyne and the fresh craters north of Maskelyne have similar ranges of CF values as Maskelyne's interior with the exception of a few units with longer CF positions.

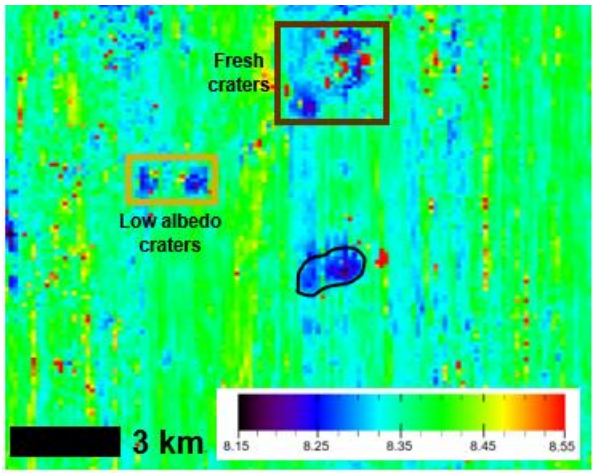

Figure 2. Diviner corrected Christiansen feature map of Maskelyne (~ 128 m / pixel resolution).

Future Work: We will compare our spectral results using different M^3 optical periods for each of the largest IMPs. We first intend to classify major compositional similarities and differences based on the IMP geological context and their morphological characteristics. This will be done via analysis of additional spectral band parameters from the M^3 data (e.g., band asymmetry), Diviner cCF maps, and the incorporation of other datasets (e.g., NAC images). This analysis will then be extended to smaller IMPs that can be spatially resolved by available M^3 and Diviner data.

References: [1] El-Baz (1973), *Apollo 17 Prelim. Sci. Rep.*, pp. 30-13 – 30-17. [2] Qiao, L. et al. (2020), *JGR* **125**, 1-26. [3] Whitaker, E.A. (1972), *Apollo 15 Prelim. Sci. Rep.*, 25-84 – 25-85. [4] Braden, S. et al. (2014), *Nature Geo.* **7** (11), 787-791. [5] Qiao, L. et al., (2017), *48th LPSC*, Abstract #1129. [6] Strain, P.L. and F. El-Baz (1980), *11th LPSC*, 2437-3446. [7] Schultz, P.H. et al. (2006), *Nature* **444** (7116), 184-186. [8] Garry, W.B. et al. (2012), *JGR* **117**, 1-15. [9] Carter et al. (2013), *44th LPSC*, Abstract #2146. [10] Qiao, L. et al. (2017), *JGR* **124**, 1100-1140. [11] Moriarty, D.M. III, and C.M. Pieters (2016), *Met. And Plan. Sci.* **51**, 207-234. [12] Greenhagen, B.T. et al. (2010), *Science* **329** (5998), 1507-1509. [13] Conel, J.E. (1969), *JGR* **74**, 1614-1634. [14] Staid, M. et al. (2011), *42nd LPSC*, Abstract #2499. [15] Bennett, K.A. et al. (2015), *46th LPSC*, Abstract #2646. [16] Donaldson Hanna, K.L. et al. (2012), *JGR* **117**. [17] Lucey et al. (2017), *Icarus* **283**, 343-351.